Supporting Information for

Four-component Relativistic ^{31}P-NMR calculations for *trans*-Platinum(II) Complexes: Importance of the Solvent and Dynamics in Spectral Simulations

Abril C. Castro,[1] Heike Fliegl,[2] Michele Cascella,[2] Trygve Helgaker,[2] Michal Repisky,[3] Stanislav Komorovsky,[3,4] María Ángeles Medrano,[5] Adoración G. Quiroga,[5] and Marcel Swart[1,6]

1. Institut de Química Computacional i Catàlisi (IQCC) & Departament de Química, Universitat de Girona, Campus Montilivi, 17003, Girona, Spain.
2. Hylleraas Centre for Quantum Molecular Sciences, Department of Chemistry, University of Oslo, P.O. Box 1033 Blindern, N-0315 Oslo, Norway.
3. Hylleraas Centre for Quantum Molecular Sciences, Department of Chemistry, University of Tromsø/ The Arctic University of Norway, N-9037 Tromsø, Norway.
4. Institute of Inorganic Chemistry, Slovak Academy of Sciences, Dúbravská cesta 9, SK-84536 Bratisla-va, Slovakia
5. Universidad Autónoma de Madrid, Dpto Química Inorgánica and Institute for Advanced Research in Chemical Sciences (IAdChem), Madrid, Spain.
6. ICREA, Pg. Lluís Companys 23, 08010, Barcelona, Spain.

Content

Computational details

All electronic-structure calculations were performed using density-functional theory (DFT). Equilibrium geometries were computed with the Amsterdam Density Functional (ADF) program,[1-2] using the QUILD program[3] with the dispersion-corrected PBE-D[4-5] functional in conjunction with uncontracted Slater-type orbital (STO) of triple-ξ quality plus double polarization functions (TZ2P).[6] The conductor-like screening model (COSMO)[7-9] was used for simulating bulk solvation in water. Scalar (SR) and spin-orbit (SO) relativistic effects were included at the two-component level using the zeroth-order regular approximation Hamiltonian (ZORA).[10-14]

The ^{31}P NMR shielding constants were calculated with the ReSpect (Relativistic Spectroscopy) program[15] and a full four-component matrix Dirac-Kohn-Sham method (mDKS) based on the Dirac-Coulomb Hamiltonian. In addition to the PBE functional, also the KT2 functional[16] was tested, as the latter is specifically designed for the calculation of NMR shielding constants and showed the best results in comparison with coupled cluster results.[17-18] The uncontracted scalar relativistic cvtz basis set of Dyall[19-21] was used for all atoms except carbon and hydrogen, for which we used the vdz basis set of Dyall. The small component basis was generated using restricted kinetic balance conditions in ground state SCF calculations whereas the restricted magnetic balance together with Gauge-Including Atomic Orbitals (GIAO) were used in the NMR shielding calculations as described in References 22 and 23.[22-23]

For comparison, quasi-relativistic SO-ZORA calculations were also performed using the ADF program, with the PBE and KT2 functionals in conjuction with the even-tempered (ET) STO-type (ET-pVQZ)[24] basis set for all atoms except platinum, for which we used the TZ2P basis set. Special STO-type basis sets (DZP, TZ2P, and QZ4P)[6] were used for the SR and SO-ZORA calculations of relativistic corrections and corresponding nonrelativistic calculations. All the shielding constants were obtained with the GIAO method.[25]

All calculated ^{31}P shielding constants σ_{calc} were converted to ^{31}P NMR chemical shifts δ_{calc} (ppm, 85% aqueous solution of H_3PO_4) using Eq. (1) as suggested by Lantto *et al.*[26] (it was -266.1 ppm in Ref. 27 and 28):[27-28]

$$\delta_{calc} = \sigma_{calc}(PH_3) - \sigma_{calc} -263.2 \text{ ppm} \qquad (1)$$

where $\sigma_{calc}(PH_3)$ is the absolute ^{31}P NMR shielding constant of phosphine (PH_3) calculated at the same level of theory and with the same basis set.

Treatment of the Solvent Effects

The experimental NMR parameters were obtained using two different types of solvent mixtures: **1)** DMSO:Acetone:H_2O(%D_2O) and **2)** DMSO:H_2O(%D_2O).

Further, for the starting *trans*-[$PtCl_2$(dma)PPh_3] complex and the PH_3 reference molecule, we performed AIMD simulations using the CP2K program package.[29] In the first system, the PH_3 molecule was solvated by 109 water molecules in a 14.6 X 14.9 X 15.3 Å^3 periodic box. The second system consisted of one *trans*-[$PtCl_2$(dma)PPh_3] molecule surrounded by 263 water molecules in a 21.0 X 19.8 X 20.7 Å^3 periodic box. The starting conformations were obtained after equilibration with 10 ns of classical molecular dynamics using the GAFF forced-field[30-31] for the solute and the TIP3P model for water.[32] Classical charges for the solute were obtained following standard RESP procedure,[33] the van der Waals parameters for Pt^{2+} were taken from the UFF.[34] During equilibration, the metallo-organic system was restrained the initial position using harmonic restraints with force constant of 5.0 kcal·mol^{-1} Å^{-2}.

After equilibration, the systems were simulated using a micro-canonical ensemble, with an average temperature of 310 K over the full trajectory. The quantum problem was treated using Kohn-Sham DFT with the PBE exchange-correlation functional,[4] in a mixed DZVP Gaussian[35] and auxiliary plane-wave (200 Ry cut-off) basis set. Core electrons were described using pseudopotentials of the

Goedecker-Teter-Hutter type.[36] Dispersion forces were taken into account using Grimme's model.[37] The simulations were extended up to 30 ps for both systems, with a time step of 0.25 fs.

As demonstrated elsewhere,[38-40] the quality of the simulation of medium effects on the shielding constants is greatly improved if the description of the solute-solvent interaction is performed with explicit solvent molecules at the quantum-mechanical level − in particular, if there is a possibility for solute-solvent hydrogen-bonding interactions. Such computations become very demanding when spectroscopic properties are calculated as averages along the AIMD trajectories. Nevertheless, as shown in the present work, it is important to perform computations with an explicit dynamic treatment of the solvent effects.

NMR studies in solution of *trans*-[$PtCl_2$(dma)PPh_3] (1).

In the case of the DMSO:water solution, the ^{31}P NMR spectra show after 30 minutes, two new signals at 18.1 and 16.5 ppm that may arise from water or DMSO coordination (see Figure S1c and S3). The ^{31}P NMR experiments with another solvent (acetone) behaves very similar to the one in DMSO:water, where again two species were present at 18 and 16 ppm (see Figure S4). The common species observed at 18,1 ppm is most likely resulting from the coordination by water, since it is not the major species in the presence of acetone (another coordinating solvent). Titration of the sample monitored by ^{1}H NMR experiments to define the aquospecies is not possible as the pH of the solution itself is basic. Several attempts to reach pH=7 using with DCl didn't change the spectra and highly hampered the measurements affording precipitation quickly.

The 2D HSQC [^{1}H-^{13}C] NMR spectra of the fresh solution show clearly no additional signals corresponding to DMSO coordination (see Figure S1b).

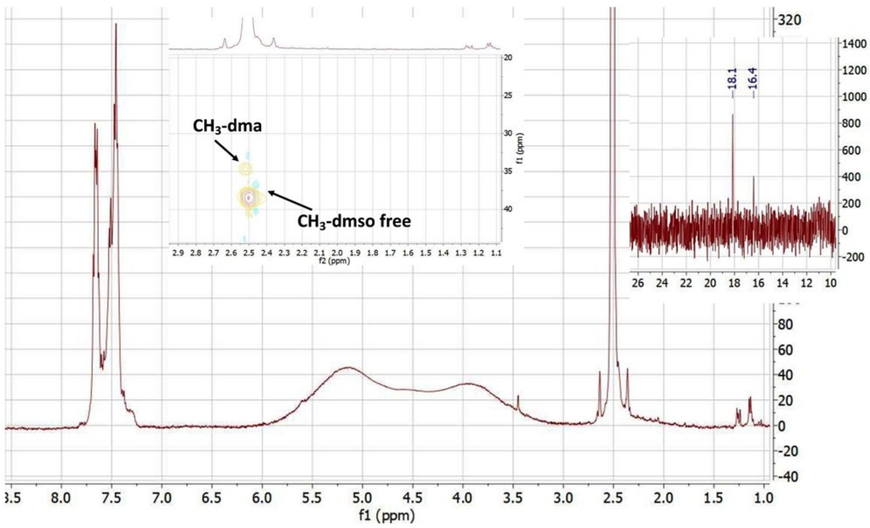

Figure S1. ^{1}H NMR, and HSQC [^{1}H-^{13}C] NMR (inset middle) and ^{31}P NMR spectra (inset right) of the complex in DMSO d_6 (200 µl) and 300 µl of D_2O/H_2O (90%/10%) after 30 min.

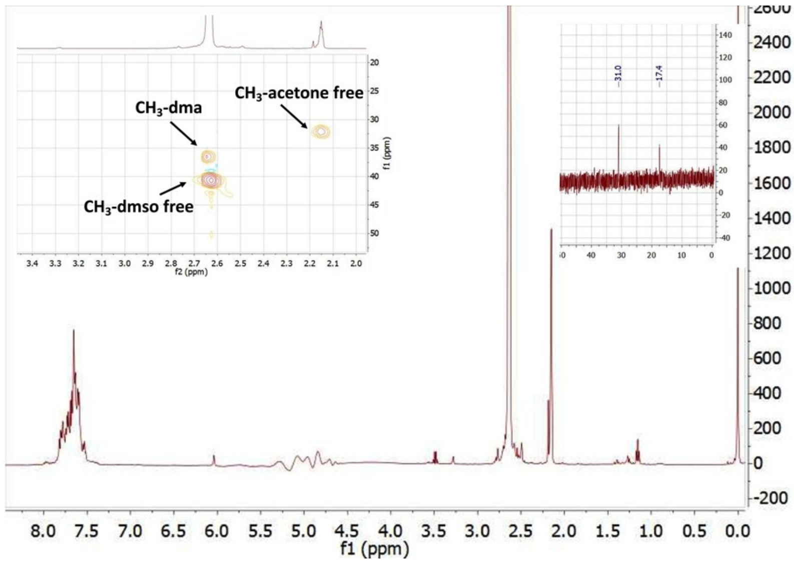

Figure S2. [1]H NMR, and HSQC [[1]H-[13]C] NMR (inset middle) and [31]P NMR spectra (inset right) of the complex in DMSO-d_6 (200 µl) and 300 µl of D_2O/H_2O/acetone (23%/66%/11%) after 4h.

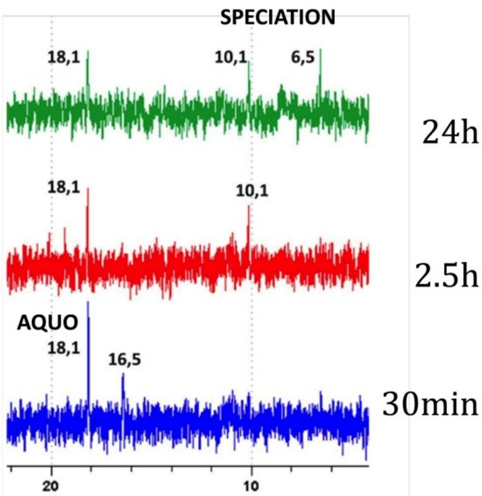

Figure S3. Extended spectra from Figure S1c. Progress of the complex in solution in DMSO-D6: D_2O/H_2O monitoring by [31]P NMR at 30min (lower), 2.5h (middle) and 24h (top).

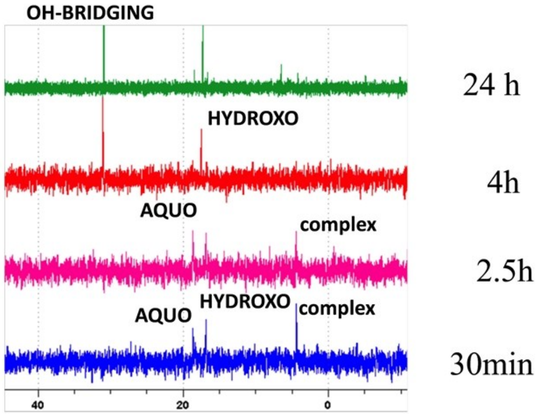

Figure S4. Extended spectra from Figure 2. Progress of the complex in solution in DMSO d_6 (200 µl) and 300 µl of D_2O/H_2O/acetone (23%/66%/11%) at 30min (lower), 2.5h (middle), 4h and 24 h (top).

Static ^{31}P NMR chemical shift calculations

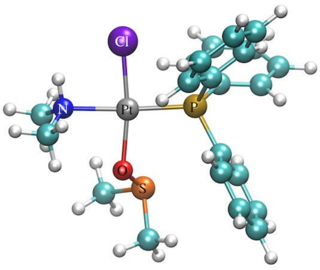

trans-[PtCl(DMSO)(PPh_3)]$^{+1}$

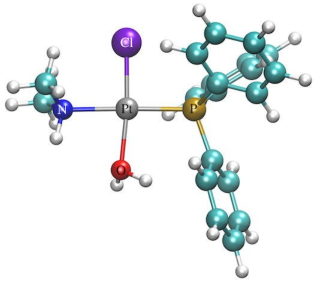

trans-[PtCl(H_2O)(PPh_3)]$^{+1}$

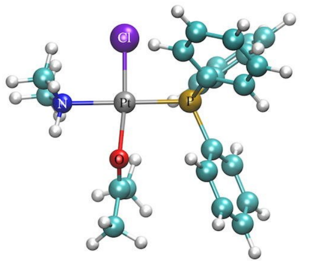

trans-[PtCl(acetone)(PPh_3)]$^{+1}$

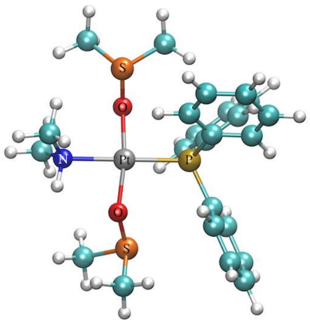

trans-[Pt($DMSO)_2$(PPh_3)]$^{+2}$

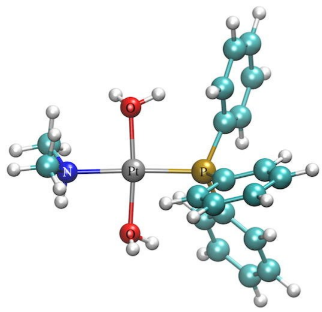

trans-[Pt($H_2O)_2$(PPh_3)]$^{+2}$

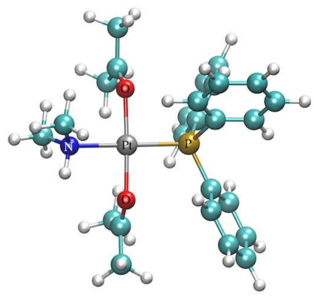

trans-[Pt(acetone$)_2$(PPh_3)]$^{+2}$

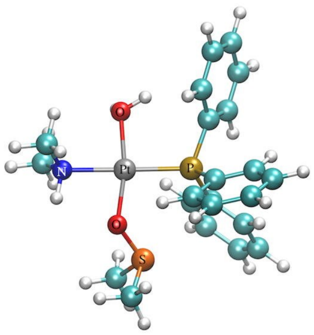

trans-[Pt(DMSO)(H_2O)(PPh_3)]$^{+2}$

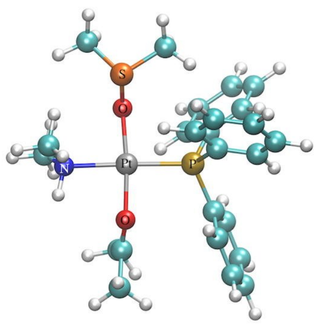

trans-[Pt(DMSO)(acetone)(PPh_3)]$^{+2}$

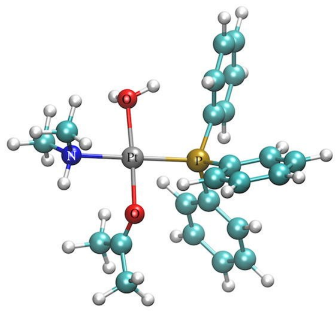

trans-[Pt(H_2O)(acetone)(PPh_3)]$^{+2}$

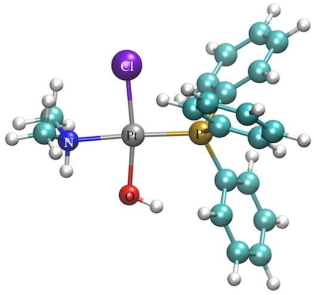

trans-[PtCl(OH)(PPh_3)]

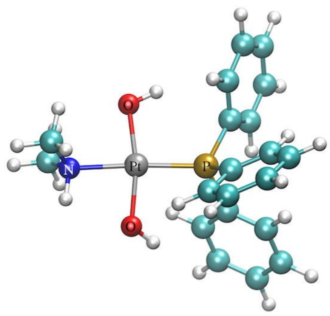

trans-[Pt($OH)_2$(PPh_3)]

Figure S5. Structures of selected *trans*-platinum(II) complexes optimized at the PBE-D/TZ2P level with COSMO.

Table S1. Basis-set dependence of ZORA relativistic corrections (SR and SO) to the ^{31}P-NMR nuclear shielding constants and chemical shifts (in ppm) of the phosphine and *trans*-platinum(II) complexes using the PBE functional.

Compounds	Basis set	Relativistic correction to nuclear shielding		Relativistic correction to chemical shift	
		SR	**SO**	**SR**	**SO**
1. Phosphine (PH_3) reference	DZP	-0.44	12.59	---	---
	TZ2P	-0.92	11.91	---	---
	ET-pVQZ	-2.27	10.29	---	---
	QZ4P	-2.14	11.21	---	---
2. trans-[$PtCl_2$(dma)(PPh_3)]	DZP	-1.93	46.15	1.49	-33.56
	TZ2P	-2.57	45.87	1.65	-33.95
	ET-pVQZ	-3.41	45.66	1.14	-35.37
	QZ4P	-2.77	46.69	0.63	-36.11
3. trans-[PtCl(DMSO)(dma)(PPh_3)]$^+$	DZP	3.05	52.53	-3.49	-39.93
	TZ2P	3.15	52.87	0.77	-40.96
	ET-pVQZ	2.25	52.77	-452	-42.48
	QZ4P	2.03	53.19	-4.17	-37.82
4. trans-[PtCl(H_2O)(dma)(PPh_3)]$^+$	DZP	3.02	46.97	-3.46	-34.37
	TZ2P	2.54	46.85	-3.46	-34.93
	ET-pVQZ	1.24	46.30	-3.51	-36.01
	QZ4P	1.71	47.19	-3.84	-32.14
5. trans-[PtCl(Acetone)(dma)(PPh_3)]$^+$	DZP	1.03	46.23	-1.48	-33.64
	TZ2P	0.78	46.25	-1.71	-34.34
	ET-pVQZ	-0.05	46.33	-2.22	-36.04
	QZ4P	0.18	46.89	-2.32	-33.36
6. trans-[$Pt(DMSO)_2$(dma)(PPh_3)]$^{2+}$	DZP	5.50	51.74	-5.95	-39.14
	TZ2P	5.84	52.44	-6.76	-40.53
	ET-pVQZ	4.99	52.33	-7.26	-42.04
	QZ4P	4.78	52.63	-6.92	-34.50
7. trans-[$Pt(H_2O)_2$(dma)(PPh_3)]$^{2+}$	DZP	10.67	53.11	-11.12	-40.52
	TZ2P	10.52	52.95	-11.44	-41.04
	ET-pVQZ	9.38	52.82	-11.65	-42.53
	QZ4P	8.95	52.71	-11.09	-30.42
8. trans-[$Pt(Acetone)_2$(dma)(PPh_3)]$^{2+}$	DZP	6.72	50.29	-7.16	-37.70
	TZ2P	6.94	50.56	-7.86	-38.65
	ET-pVQZ	6.00	50.73	-8.27	-40.44
	QZ4P	5.65	50.43	-7.79	-31.43
9. Pt(DMSO)(H_2O)(dma)(PPh_3)$^{2+}$	DZP	7.19	50.05	-7.63	-37.46
	TZ2P	7.11	50.04	-8.03	-38.13
	ET-pVQZ	6.12	50.08	-8.39	-39.78
	QZ4P	5.80	49.41	-7.94	-30.27
10. trans-[Pt(DMSO)(Acetone)(dma)(PPh_3)]$^{2+}$	DZP	5.45	50.53	-5.90	-37.94
	TZ2P	5.77	51.10	-6.69	-39.19
	ET-pVQZ	5.02	51.14	-7.29	-40.85
	QZ4P	4.58	51.20	-6.72	-33.27
11. trans-[Pt(H_2O)(Acetone)(dma)(PPh_3)]$^{2+}$	DZP	8.48	51.59	-8.92	-39.00
	TZ2P	8.64	51.78	-9.56	-39.86
	ET-pVQZ	7.65	51.80	-9.92	-41.51
	QZ4P	7.14	51.61	-9.28	-31.13

Table S2. Basis-set dependence of ZORA relativistic corrections (SR and SO) to the ^{31}P-NMR nuclear shielding constants and chemical shifts (in ppm) of the phosphine and *trans*-platinum(II) complexes using the KT2 functional.

Compounds	Basis set	Relativistic correction to nuclear shielding		Relativistic correction to chemical shift	
		SR	SO	SR	SO
1. Phosphine (PH_3) reference	DZP	-0.33	12.78	---	---
	TZ2P	-0.83	12.09	---	---
	ET-pVQZ	-2.08	10.59	---	---
	QZ4P	-2.04	11.35	---	---
2. trans-[$PtCl_2$(dma)(PPh_3)]	DZP	-1.66	46.22	1.33	-33.43
	TZ2P	-2.33	45.77	1.50	-33.68
	ET-pVQZ	-3.03	45.65	0.95	-35.06
	QZ4P	-2.50	46.56	0.46	-35.66
3. trans-[PtCl(DMSO)(dma)(PPh_3)]$^+$	DZP	3.14	52.21	-3.47	-39.42
	TZ2P	3.19	52.36	-1.64	-40.27
	ET-pVQZ	2.43	52.31	1.98	-41.73
	QZ4P	2.13	52.65	-4.17	-37.12
4. trans-[PtCl(H_2O)(dma)(PPh_3)]$^+$	DZP	3.14	46.65	-3.47	-33.86
	TZ2P	2.63	46.40	-3.46	-34.30
	ET-pVQZ	1.77	46.23	-3.85	-35.64
	QZ4P	1.85	46.70	-3.89	-31.46
5. trans-[PtCl(Acetone)(dma)(PPh_3)]$^+$	DZP	1.23	46.10	-1.56	-33.32
	TZ2P	0.93	45.96	-1.76	-33.87
	ET-pVQZ	0.22	46.10	-2.31	-35.51
	QZ4P	0.37	46.58	-2.41	-32.82
6. trans-[Pt$(DMSO)_2$(dma)(PPh_3)]$^{2+}$	DZP	5.44	50.72	-5.77	-37.94
	TZ2P	5.70	51.17	-6.53	-39.08
	ET-pVQZ	5.00	51.13	-7.08	-40.54
	QZ4P	4.71	51.31	-6.75	-33.21
7. trans-[Pt$(H_2O)_2$(dma)(PPh_3)]$^{2+}$	DZP	10.41	52.10	-10.74	-39.31
	TZ2P	10.19	51.80	-11.02	-39.70
	ET-pVQZ	9.20	51.72	-11.29	-41.14
	QZ4P	8.72	51.57	-10.77	-29.45
8. trans-[Pt$(Acetone)_2$(dma)(PPh_3)]$^{2+}$	DZP	6.84	49.81	-7.17	-37.03
	TZ2P	6.95	49.89	-7.78	-37.80
	ET-pVQZ	6.13	50.08	-8.21	-39.50
	QZ4P	5.72	49.73	-7.76	-30.62
9. Pt(DMSO)(H_2O)(dma)(PPh_3)$^{2+}$	DZP	7.09	49.22	-7.43	-36.44
	TZ2P	6.98	49.05	-7.81	-36.96
	ET-pVQZ	6.11	49.12	-8.19	-38.54
	QZ4P	5.73	48.40	-7.78	-29.28
10. trans-[Pt(DMSO)(Acetone)(dma)(PPh_3)]$^{2+}$	DZP	5.46	49.80	-5.79	-37.02
	TZ2P	5.68	50.12	-6.51	-38.03
	ET-pVQZ	5.06	50.21	-7.14	-39.63
	QZ4P	4.55	50.18	-6.59	-32.24
11. trans-[Pt(H_2O)(Acetone)(dma)(PPh_3)]$^{2+}$	DZP	8.46	50.91	-8.79	-38.12
	TZ2P	8.54	50.91	-9.37	-38.82
	ET-pVQZ	7.69	51.00	-9.77	-40.41
	QZ4P	7.12	50.73	-9.16	-30.21

Table S3. Basis-set dependence of mDKS relativistic corrections to the ^{31}P NMR nuclear shielding constants and chemical shifts (in ppm) of the parent *trans*-[$PtCl_2$(dma)PPh_3] complex.

dyall_vdz	dyall_cvtz	^{31}P NMR shielding (σ)	^{31}P NMR shift (δ)
All atoms	---	326.92	16.7
Pt, Cl, N, C, H	P	282.39	38.2
Cl, N, C, H	P, Pt	282.31	38.3
C, H	P, Pt, Cl, N	282.07	38.5

Table S4. Dynamically calculated ^{31}P NMR shielding constants σ (in ppm) of complex 1 with explicit water molecules obtained with four-component relativistic methods.

	Average σ values (^{31}P)	
	mDKS-PBE	mDKS-KT2
Isolated complex	285.3 ± 9.0	330.7 ± 8.8
Explicit 3 water molecules	285.5 ± 8.8	330.8 ± 8.7
Explicit 5 water molecules	285.7 ± 8.9	330.9 ± 8.7

[a] Calculated using the dyall_cvtz basis set.

Table S5. Static and dynamic 31P-NMR chemical shifts of the complex 1.

		Reference(PH_3) shielding(σ)	Complex Shielding(σ)	Correction value	Shift (δ)
	Experimental shift value	---	---	---	4.4
	SO-ZORA/PBE[a]				
Static- Gas phase	Isolated complex	590.5	282.0	-263.2	45.3
Static- COSMO	Isolated complex	589.9	283.2	-263.2	43.5
Static- Gas phase	Explicit 3 water molecules	590.5	284.9	-263.2	42.4
Dynamic	Isolated complex	584.7 ± 15.6	283.5 ± 8.4	-263.2	38.0
Dynamic	Explicit 3 water molecules	584.7 ± 15.6	284.3 ± 8.3	-263.2	37.2
Dynamic	Explicit 5 water molecules	584.7 ± 15.6	284.6 ± 8.3	-263.2	36.9
	SO-ZORA/KT2[a]				
Static- Gas phase	Isolated complex	617.5	336.7	-263.2	17.6
Static- COSMO	Isolated complex	617.2	337.7	-263.2	16.3
Static- Gas phase	Explicit 3 water molecules	617.5	336.8	-263.2	17.5
Dynamic	Isolated complex	612.0 ± 14.8	337.2 ± 7.9	-263.2	11.6
Dynamic	Explicit 3 water molecules	612.0 ± 14.8	336.5 ± 7.7	-263.2	12.3
Dynamic	Explicit 5 water molecules	612.0 ± 14.8	336.7 ± 7.7	-263.2	12.1

[a] Calculated with the TZ2P basis set.

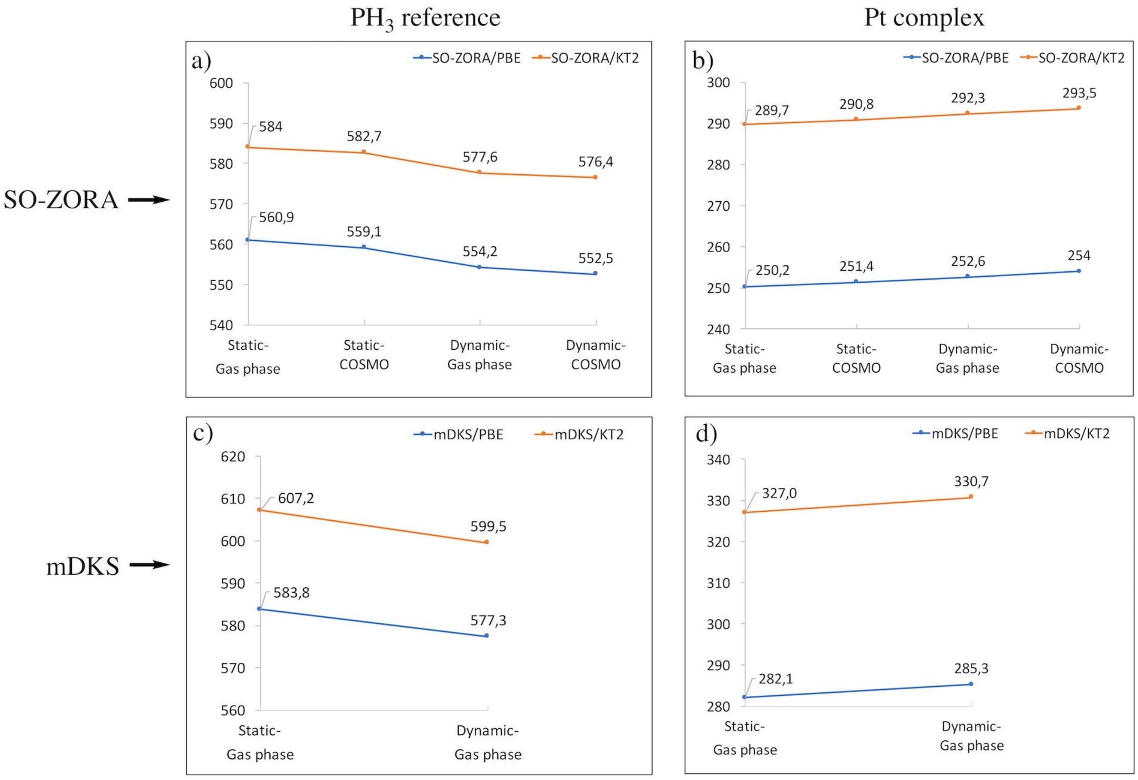

Figure S6. Dynamically calculated [31]P-NMR shielding (σ) constants of the PH_3 and *trans*-[$PtCl_2$(dma)PPh_3] complex obtained with SO-ZORA (Gas-phase and aqueous solution) (a-b) and mDKS (c-d) relativistic corrections at the PBE (in blue) and KT2 (in orange) levels.

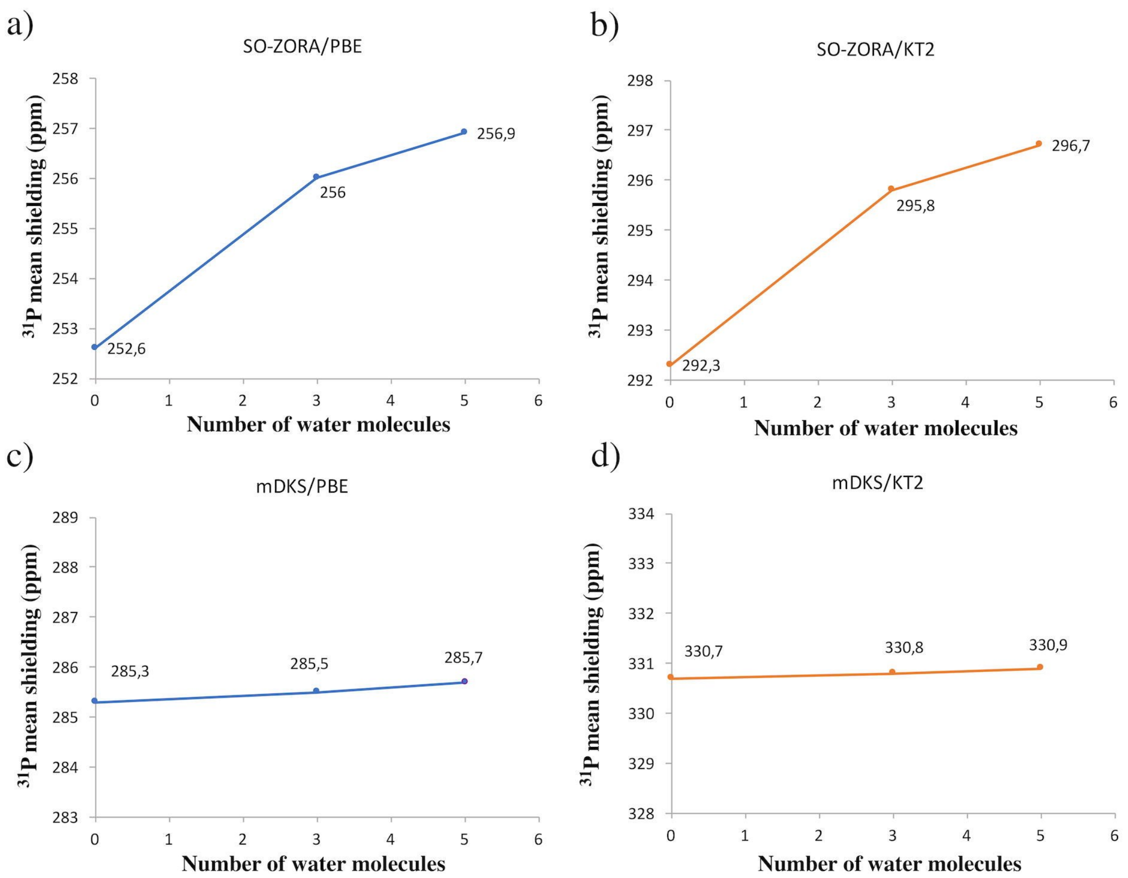

Figure S7. Dynamically calculated ^{31}P-NMR shielding constants σ (in ppm) of the *trans*-[$PtCl_2$(dma)PPh_3] with explicit water molecules obtained with SO-ZORA (a-b) and mDKS (c-d) relativistic corrections at the PBE (in blue) and KT2 (in orange) levels.

Table S6. Dynamically calculated ^{31}P-NMR chemical shielding (σ) constants of the PH_3 obtained at the SO-ZORA level and using the PBE and KT2 functionals.

	SO-ZORA/PBE		**SO-ZORA/KT2**	
Snapshots	Gas-phase	*COSMO*	Gas-phase	*COSMO*
1	545.3	543.4	568.9	567.5
2	590.0	588.0	612.3	610.7
3	565.0	563.1	588.1	586.6
4	531.6	530.2	555.5	554.6
5	553.0	551.6	576.6	575.7
6	531.7	530.9	556.4	556.0
7	561.9	559.5	584.4	582.5
8	555.7	554.5	579.6	578.8
9	566.6	564.7	589.2	587.8
10	527.9	527.3	552.9	552.6
11	568.9	566.8	591.6	590.0
12	543.8	542.3	567.8	566.7
13	567.5	565.5	590.4	589.0
14	563.9	562.4	587.3	586.3
15	538.5	537.3	563.3	562.6
16	544.8	543.1	568.5	567.3
17	536.0	534.5	559.8	558.9
18	536.5	535.4	561.0	560.3
19	564.2	562.2	587.2	585.6
20	546.1	544.6	569.7	568.8
21	580.7	578.4	602.9	601.2
22	575.7	573.2	597.8	595.8
23	557.8	556.3	581.3	580.3
24	570.4	568.5	593.2	591.8
25	559.0	556.5	581.7	579.8
26	564.1	562.4	587.7	586.5
27	575.7	573.3	597.8	596.0
28	524.9	524.2	549.5	549.2
29	554.4	552.6	577.7	576.3
30	523.1	522.3	548.1	547.8
AVERAGE	554.2	552.5	577.6	576.4
STANDARD DEVIATION	17.6	17.2	16.8	16.4

Figure S8. Plot of the dynamically calculated ^{31}P-NMR chemical shielding (σ) constants of the PH_3 reported in Table S6.

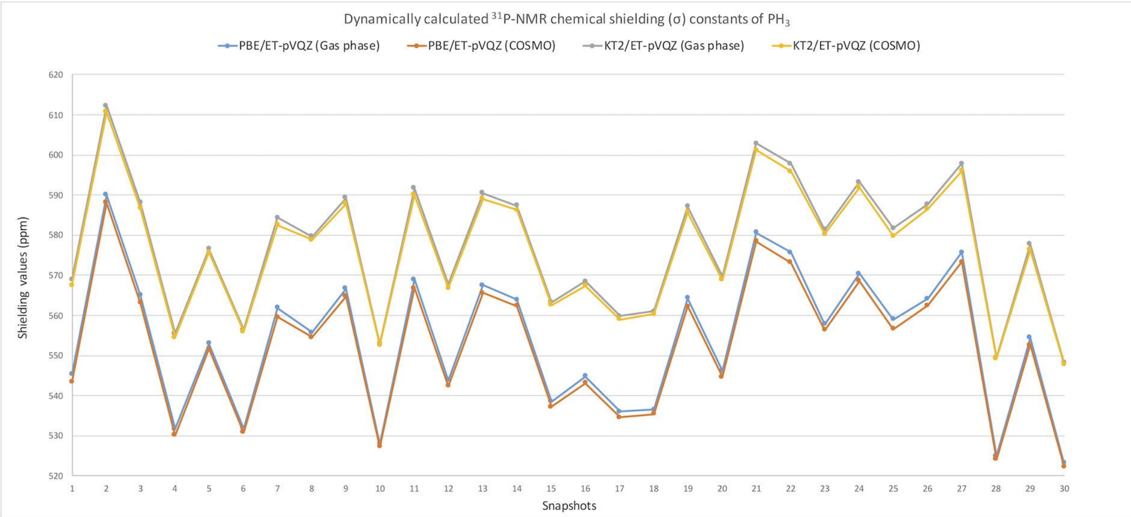

Table S7. Dynamically calculated ^{31}P-NMR chemical shielding (σ) constants of the *trans*-[$PtCl_2$(dma)PPh_3] obtained at the SO-ZORA level and using the PBE and KT2 functionals.

	SO-ZORA/PBE				SO-ZORA/KT2			
Snapshots	Isolated (Gas-phase)	Isolated (COSMO)	*Pt complex* + 3 water	*Pt complex* + 5 water	Isolated (Gas-phase)	Isolated (COSMO)	*Pt complex* + 3 water	*Pt complex* + 5 water
1	239.8	241.3	242.4	242.7	279.2	280.5	281.8	281.8
2	260.6	261.4	263.4	263.4	300.8	301.6	303.5	303.3
3	256.6	257.5	260.7	261.2	295.8	296.7	300.0	300.7
4	266.9	267.0	267.8	267.9	306.4	306.5	307.2	307.2
5	249.8	250.7	251.6	251.4	289.3	290.2	291.5	291.0
6	254.5	255.9	255.8	256.2	294.4	295.7	295.5	295.8
7	257.2	259.6	260.4	260.0	297.0	299.3	300.1	299.7
8	258.5	260.6	259.8	259.1	298.1	300.1	299.3	298.4
9	264.9	267.1	267.5	268.6	304.3	306.4	306.8	308.0
10	245.6	248.4	247.0	247.7	286.1	288.6	287.1	287.9
11	243.1	244.4	244.8	247.4	283.0	284.1	284.3	287.1
12	247.3	249.4	250.9	251.2	286.8	288.9	290.7	290.9
13	253.2	254.8	255.9	259.0	294.1	295.6	296.4	299.6
14	253.5	256.4	256.7	257.7	292.5	295.2	295.6	296.5
15	266.0	266.6	267.9	269.2	305.7	306.1	307.6	308.8
16	251.5	252.4	252.5	253.6	291.1	292.0	291.9	293.0
17	237.0	239.3	240.6	240.8	277.5	279.6	281.3	281.3
18	251.9	252.8	254.2	256.1	291.8	292.6	293.9	295.9
19	264.1	264.8	269.4	270.5	303.3	303.8	309.1	309.9
20	254.3	253.8	261.3	261.8	293.6	293.1	301.1	301.8
21	238.9	239.4	244.1	243.5	279.8	280.2	285.7	285.0
22	260.7	262.3	266.6	268.2	299.8	301.1	306.1	307.9
23	250.1	251.2	254.2	254.6	290.8	291.6	295.2	295.6
24	260.6	261.6	267.3	269.1	299.2	300.1	306.6	308.3
25	257.7	258.7	262.8	263.1	297.0	297.8	302.8	303.2
26	256.3	256.4	262.5	263.8	295.1	295.1	302.3	303.6
27	261.7	263.1	266.2	267.5	300.3	301.4	304.8	306.3
28	237.2	237.8	238.2	237.9	276.5	277.2	277.3	277.0
29	240.8	243.0	244.2	245.3	280.6	282.6	283.8	284.9
30	237.8	240.7	244.2	247.0	277.6	280.3	284.3	290.8
AVERAGE	**252.6**	**253.9**	**256.0**	**256.8**	**292.3**	**293.5**	**295.8**	**296.7**
STANDARD DEVIATION	9.2	8.9	9.5	9.6	8.9	8.7	9.3	9.3

Figure S9. Plot of the dynamically calculated ^{31}P-NMR chemical shielding (σ) constants of the *trans*-[$PtCl_2$(dma)PPh_3] complex reported in Table S7.

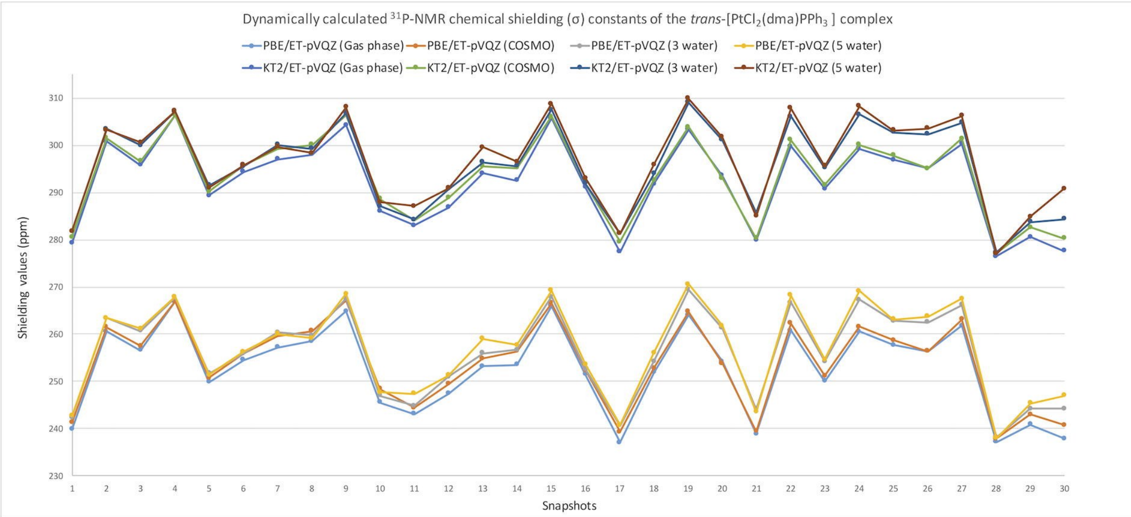

Table S8. Dynamically calculated ^{31}P-NMR chemical shielding (σ) constants of the *trans*-[$PtCl_2$(dma)PPh_3] obtained at the mDKS level and using the PBE and KT2 functionals.

	mDKS/PBE			**mDKS/KT2**		
Snapshots	Isolated (Gas-phase)	*Pt complex* + 3 water	*Pt complex* + 5 water	Isolated (Gas-phase)	*Pt complex* + 3 water	*Pt complex* + 5 water
1	272.9	274.0	273.9	318.4	319.4	319.3
2	290.8	292.7	293.3	336.7	338.5	338.9
3	286.6	288.6	288.4	331.5	333.3	333.1
4	300.3	301.2	300.7	345.9	346.6	346.1
5	283.4	282.9	283.3	328.8	328.5	328.8
6	286.3	286.1	286.7	331.9	331.6	332.1
7	290.2	291.6	291.5	335.6	336.7	336.7
8	287.1	287.5	287.6	331.8	332.2	332.1
9	295.6	297.1	297.1	340.3	341.8	341.7
10	280.1	281.6	281.0	326.9	328.4	327.9
11	274.0	275.6	276.2	319.3	320.8	321.2
12	281.8	282.2	282.3	327.1	327.4	327.4
13	284.3	285.6	286.0	330.9	331.9	332.2
14	285.5	286.6	287.1	330.0	331.1	331.3
15	297.7	298.0	298.7	343.1	343.2	343.6
16	282.6	283.2	282.6	327.6	328.0	327.5
17	270.5	270.8	270.7	316.8	316.9	316.6
18	283.6	285.2	284.9	329.0	330.5	329.9
19	299.3	297.7	298.4	344.6	342.8	343.3
20	288.8	286.2	285.7	334.0	331.0	330.5
21	271.6	269.3	269.3	317.8	315.4	315.2
22	295.4	293.9	294.2	340.5	338.7	339.0
23	284.1	284.1	284.4	331.1	331.0	331.2
24	293.2	292.2	293.5	337.3	336.2	337.3
25	290.5	289.3	289.2	335.7	334.4	334.3
26	290.9	288.1	287.9	336.0	333.0	332.7
27	295.9	295.8	296.1	340.5	340.2	340.5
28	269.1	269.2	269.3	314.0	314.0	314.1
29	275.2	277.3	277.7	321.3	323.1	323.5
30	272.3	272.4	273.5	317.9	317.8	318.8
AVERAGE	**285.3**	**285.5**	**285.7**	**330.7**	**330.8**	**330.9**
STANDARD DEVIATION	9.0	8.9	8.9	8.8	8.7	8.7

Figure S10. Plot of the dynamically calculated ^{31}P-NMR chemical shielding (σ) constants of the *trans*-$[PtCl_2(dma)PPh_3]$ complex reported in Table S8.

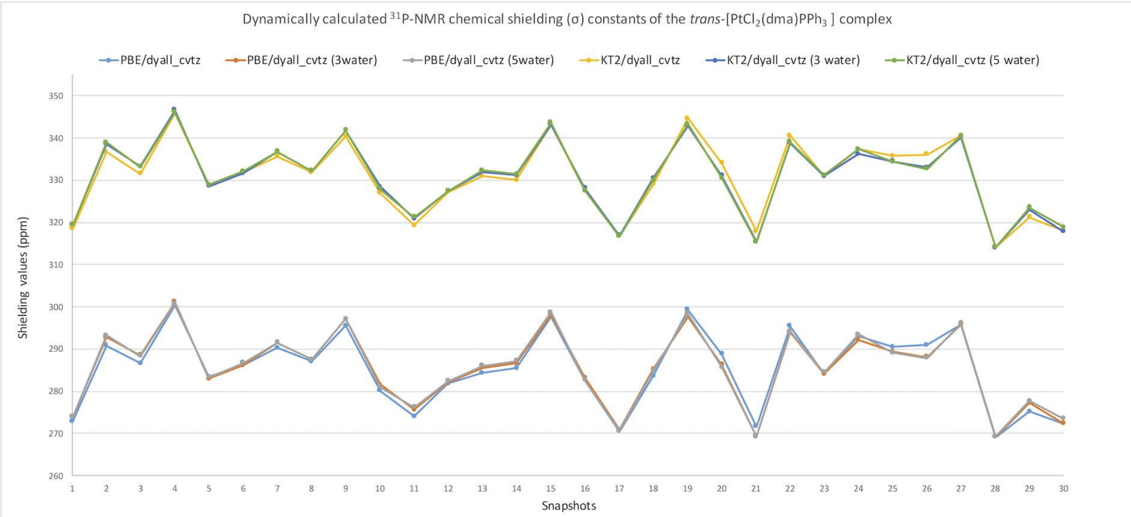

Radial distribution functions from AIMD simulations

Indication for the need of an explicit solvent model is given by the presence of weakly bound water molecules along the axial region of the platinum complex. The analysis of the Pt-O radial distribution function (RDF) shows that the Pt ion is mostly screened from the solvent by its bulky ligands. The small peak at 3.9 Å (see Figure S2a) reveals nonetheless the statistical presence of one water molecule weakly bound to the platinum along the principal symmetry axis of the square-planar ligand. Furthermore, the peak around 2.5 Å in the Pt-H RDF (see Figure S2b) support the possible presence of a solvent-assisted "inverse" or "anionic" hydration previously observed in square-planar aqua ions such as $[Pt(H_2O)_4]^{2+}$ and solvated $[PtX_4]^{2-}$ (X = Cl, Br, CN) complexes.[39, 41-42] The authors have shown that the axial Pt←H_2O and Pt←OH_2 interactions are involved in the presence of water molecules in the nonequatorial regions of the Pt(II) complexes. Interestingly, it was demonstrated that the presence of such axial water molecules is mainly induced by the surrounding bulk water and that this effect cannot be properly recovered by using static quantum molecular approach.[43]

Figure S11. Radial distribution function of the water a) oxygen and b) hydrogen atoms around Pt a for the solvated *trans*-[$PtCl_2$(dma)PPh_3] complex. The arrows describe the statistical presence of a weakly bound water along the axis perpendicular to the square-planar Pt complex.

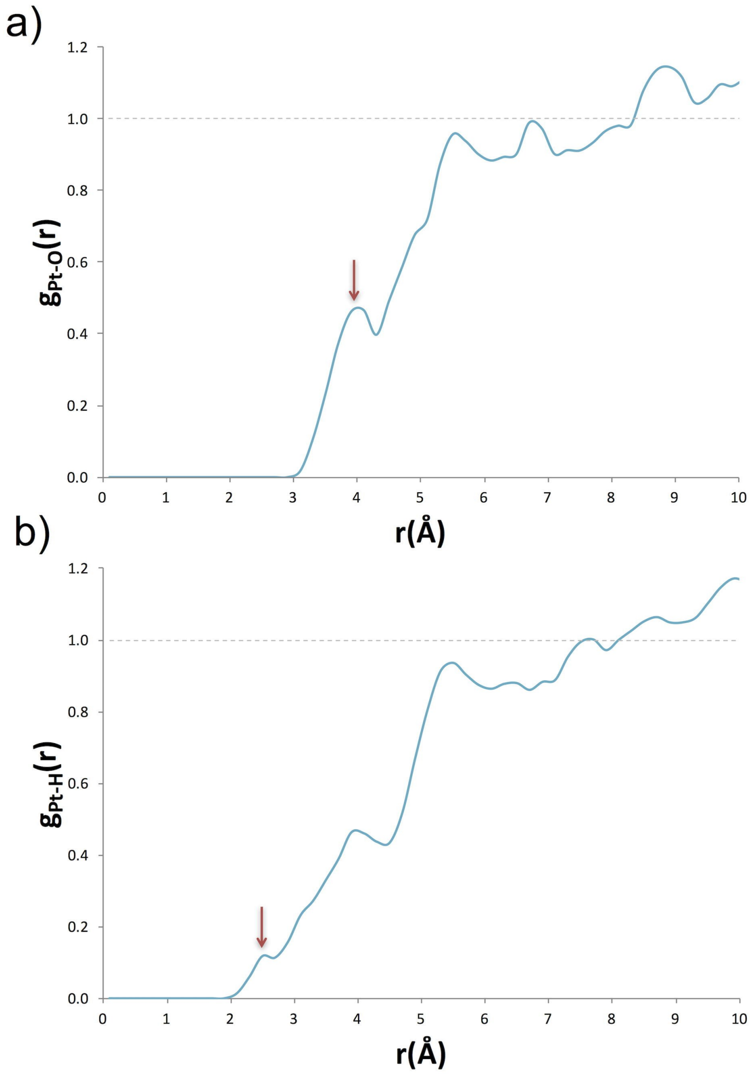

References

(1) te Velde, G.; Bickelhaupt, F. M.; Baerends, E. J.; Fonseca Guerra, C.; van Gisbergen, S. J. A.; Snijders, J. G.; Ziegler, T., *J. Comput. Chem.* **2001,** *22* (9), 931-967.

(2) Baerends, E. J.; Ziegler, T.; Atkins, A. J.; Autschbach, J.; Bashford, D.; Bérces, A.; Bickelhaupt, F. M.; Bo, C.; Boerrigter, P. M.; Cavallo, L.; Chong, D. P.; Chulhai, D. V.; Deng, L.; Dickson, R. M.; Dieterich, J. M.; Ellis, D. E.; Faassen, M. v.; Fan, L.; Fischer, T. H.; Fonseca Guerra, C.; Franchini, M.; Ghysels, A.; Giammona, A.; van Gisbergen, S. J. A.; Götz, A. W.; Groeneveld, J. A.; Gritsenko, O. V.; Grüning, M.; Gusarov, S.; Harris, F. E.; Heine, T.; van den Hoek, P.; Jacob, C. R.; Jacobsen, H.; Jensen, L.; Kaminski, J. W.; van Kessel, G.; Kootstra, F.; Kovalenko, A.; Krykunov, M. V.; van Lenthe, E.; McCormack, D. A.; Michalak, A.; Mitoraj, M.; Morton, S. M.; Neugebauer, J.; Nicu, V. P.; Noodleman, L.; Osinga, V. P.; Patchkovskii, S.; Pavanello, M.; Peeples, C. A.; Philipsen, P. H. T.; Post, D.; Pye, C. C.; Ravenek, W.; Rodríguez, J. I.; Ros, P.; Rüger, R.; Schipper, P. R. T.; van Schoot, H.; Schreckenbach, G.; Seldenthuis, J. S.; Seth, M.; Snijders, J. G.; Solà, M.; Swart, M.; Swerhone, D.; te Velde, G.; Vernooijs, P.; Versluis, L.; Visscher, L.; Visser, O.; Wang, F.; Wesolowski, T. A.; van Wezenbeek, E. M.; Wiesenekker, G.; Wolff, S. K.; Woo, T. K.; Yakovlev, A. L. *ADF2016*, ADF2016.01; SCM, Theoretical Chemistry, Vrije Universiteit: Amsterdam, 2016.

(3) Swart, M.; Bickelhaupt, F. M., *J. Comput. Chem.* **2008,** *29* (5), 724-734.

(4) Perdew, J. P.; Burke, K.; Ernzerhof, M., *Phys. Rev. Lett.* **1996,** *77* (18), 3865-3868.

(5) Grimme, S., *J. Comput. Chem.* **2006,** *27* (15), 1787-1799.

(6) Van Lenthe, E.; Baerends, E. J., *J. Comput. Chem.* **2003,** *24* (9), 1142-1156.

(7) Klamt, A.; Schüürmann, G., *J. Chem. Soc. Perkin Trans. 2* **1993,** (5), 799-805.

(8) Klamt, A., *J. Phys. Chem.* **1996,** *100* (9), 3349-3353.

(9) Pye, C. C.; Ziegler, T., *Theor. Chem. Acc.* **1999,** *101* (6), 396-408.

(10) van Lenthe, E.; Ehlers, A.; Baerends, E.-J., *J. Chem. Phys.* **1999,** *110* (18), 8943-8953.

(11) van Lenthe, E.; Baerends, E. J.; Snijders, J. G., *J. Chem. Phys.* **1993,** *99* (6), 4597-4610.

(12) van Lenthe, E.; Baerends, E. J.; Snijders, J. G., *J. Chem. Phys.* **1994,** *101* (11), 9783-9792.

(13) van Lenthe, E.; Snijders, J. G.; Baerends, E. J., *J. Chem. Phys.* **1996,** *105* (15), 6505-6516.

(14) van Lenthe, E.; van Leeuwen, R.; Baerends, E. J.; Snijders, J. G., *Int. J. Quantum Chem* **1996,** *57* (3), 281-293.

(15) Repiský, M.; Komorovský, S.; Malkin, V. G.; Malkina, O. L.; Kaupp, M.; Ruud, K.; with contributions from Bast, R.; Ekström, U.; Kadek, M.; Knecht, S.; Konecny, L.; Malkin, E.; Malkin-Ondik, I. *ReSpect, Relativistic Spectroscopy DFT program*, ReSpect, Relativistic Spectroscopy DFT program (see http://www.respectprogram.org/), version 4.0.0; 2016.

(16) Keal, T. W.; Tozer, D. J., *J. Chem. Phys.* **2003,** *119* (6), 3015-3024.

(17) Teale, A. M.; Lutnæs, O. B.; Helgaker, T.; Tozer, D. J.; Gauss, J., *J. Chem. Phys.* **2013,** *138* (2), 024111.

(18) Reimann, S.; Ekström, U.; Stopkowicz, S.; Teale, A. M.; Borgoo, A.; Helgaker, T., *Phys. Chem. Chem. Phys.* **2015,** *17* (28), 18834-18842.

(19) K. G. Dyall, unpublished; available from web site, http://dirac.chem.sdu.dk/.

(20) Dyall, K. G., *Theor. Chem. Acc.* **2004,** *112* (5), 403-409.

(21) Gomes, A. S. P.; Dyall, K. G.; Visscher, L., *Theor. Chem. Acc.* **2010,** *127* (4), 369-381.

(22) Komorovský, S.; Repiský, M.; Malkina, O. L.; Malkin, V. G.; Ondík, I. M.; Kaupp, M., *J. Chem. Phys.* **2008,** *128* (10), 104101.

(23) Komorovský, S.; Repiský, M.; Malkina, O. L.; Malkin, V. G., *J. Chem. Phys.* **2010,** *132* (15), 154101.

(24) Chong, D. P.; Van Lenthe, E.; Van Gisbergen, S.; Baerends, E. J., *J. Comput. Chem.* **2004,** *25* (8), 1030-1036.

(25) Ditchfield, R., *Mol. Phys.* **1974,** *27* (4), 789-807.

(26) Lantto, P.; Jackowski, K.; Makulski, W.; Olejniczak, M.; Jaszuński, M., *J. Phys. Chem. A* **2011,** *115* (38), 10617-10623.

(27) Jameson, C. J.; De Dios, A.; Keith Jameson, A., *Chem. Phys. Lett.* **1990,** *167* (6), 575-582.

(28) van Wüllen, C., *Phys. Chem. Chem. Phys.* **2000,** *2* (10), 2137-2144.

(29) CP2K Developers Group *CP2K Developers Group,* http://www.cp2k.org/ *(accessed Sep 2, 2016)*, ed. 2016.

(30) Wang, J.; Wolf, R. M.; Caldwell, J. W.; Kollman, P. A.; Case, D. A., *J. Comput. Chem.* **2004,** *25* (9), 1157-1174.

(31) Wang, J.; Wang, W.; Kollman, P. A.; Case, D. A., *Journal of Molecular Graphics and Modelling* **2006,** *25* (2), 247-260.

(32) Jorgensen, W. L.; Chandrasekhar, J.; Madura, J. D.; Impey, R. W.; Klein, M. L., *J. Chem. Phys.* **1983,** *79* (2), 926-935.

(33) Bayly, C. I.; Cieplak, P.; Cornell, W.; Kollman, P. A., *J. Phys. Chem.* **1993,** *97* (40), 10269-10280.

(34) Rappe, A. K.; Casewit, C. J.; Colwell, K. S.; Goddard, W. A.; Skiff, W. M., *J. Am. Chem. Soc.* **1992,** *114* (25), 10024-10035.

(35) Godbout, N.; Salahub, D. R.; Andzelm, J.; Wimmer, E., *Can. J. Chem.* **1992,** *70* (2), 560-571.

(36) Goedecker, S.; Teter, M.; Hutter, J., *Phys. Rev. B* **1996,** *54* (3), 1703-1710.

(37) Grimme, S.; Antony, J.; Ehrlich, S.; Krieg, H., *J. Chem. Phys.* **2010,** *132* (15), 154104.

(38) Sterzel, M.; Autschbach, J., *Inorg. Chem.* **2006,** *45* (8), 3316-3324.

(39) Truflandier, L. A.; Autschbach, J., *J. Am. Chem. Soc.* **2010,** *132* (10), 3472-3483.

(40) Autschbach, J.; Le Guennic, B., *Chem. Eur. J.* **2004,** *10* (10), 2581-2589.

(41) Beret, E. C.; Pappalardo, R. R.; Doltsinis, N. L.; Marx, D.; Sánchez Marcos, E., *ChemPhysChem* **2008,** *9* (2), 237-240.

(42) Beret, E. C.; Martínez, J. M.; Pappalardo, R. R.; Marcos, E. S.; Doltsinis, N. L.; Marx, D., *J. Chem. Theory Comp.* **2008,** *4* (12), 2108-2121.

(43) Truflandier, L. A.; Sutter, K.; Autschbach, J., *Inorg. Chem.* **2011,** *50* (5), 1723-1732.